Image optimization for a linear CPV system

A. Giannuzzi, P. Sansoni, D. Fontani, F. Francini, D. Jafrancesco, L. Mercatelli, E. Sani
CNR-INOA National Institute of Applied Optics, L.go E. Fermi, 6, 50125 Firenze, Italy
alessandra.giannuzzi@inoa.it

Abstract

Linear Concentrating PhotoVoltaic systems mostly are solar troughs with parabolic profile. The advantage of this configuration is basically due to its simplicity of fabrication and of working principle. Solar trough collectors are usually employed in thermal applications using as absorber a metal pipe. When the receiver is a cell array, collection efficiency maximization must be combined to light distribution requirements of the PV cell. The trough system is simulated on the base on the experimentation realized on a prototype of solar CPV trough with parabolic profile. The paper examines the influence of mirror focal length, mirror deformation and absorber position on the light distribution over the receiver. The simulations show how large is the influence of some parameters on the total power collected by every single cell. The analysis is addressed to optimize a parabolic trough PV/thermal collector with a geometric concentration ratio around 150.

Keywords Solar troughs; Concentration; Optical performance.

1. Introduction

It is a common use to associate the idea of a parabolic trough collector exclusively to the production of thermal energy. In general thermal and photovoltaic systems are completely different approaches to exploit solar energy. For instance, in photovoltaics (PV), the cell temperature must be kept as low as possible because the cell conversion efficiency decreases with the temperature [1]. Moreover, receiver geometry and precision of image formation are usually different in the two approaches [2]. Our study is devoted to evaluate the optical performance of a linear system conceived for producing electricity, but with cool cogeneration. This additional function is obtained exploiting the light that is not directly focused on the cells, which contributes to heat in cogeneration a fluid contained in a cooling element. So the optical performance of the whole system has to be evaluated taking into account that the light not directly converted in electricity can be recovered in a thermal cycle.

The examined CPV (Concentrating PhotoVoltaic) system is specially conceived for residential purposes. It is composed of a linear parabolic mirror concentrating the sunlight over an array of PV cells with a geometric concentration factor of circa 150 (excluding the shading due to the receiver). In the framework of the "CESARE" project (Concentrated pv combinEd SolAR Energy system), the construction of a first prototype is currently under development at the Energetic Engineering Dept. of the University of Florence (Italy) in collaboration with the National Institute of Optics of the National Research Council (CNR-INO). The collecting mirror is realized in metal, while the selected cells are high efficiency PV cells, of square or rectangular shape, with lateral dimensions in the range 7mm -10mm.

For such a system the aim is to produce both thermal and electrical energy in order to completely exploit all the light concentrated by the primary mirror, in particular recovering also the portion focused outside the cells array [3]. The cells temperature increases with the concentrating factor and consequently they need to be cooled. An heat exchanger, such as a pipe containing a fluid, must be coupled to the cells both for cooling them and for a successive reuse (for example to provide sanitary hot water or being addressed to other processes) of the heat stored in the fluid. The paper presents a preliminary study representing a first approach to understand how light concentrated from a parabolic trough system is affected by the single parameters of the trough. The examined parameters are: the focal length, receiver defocusing, rigid mirror deformations.

2. Energy distribution dependence on focal length

The development of Concentrating PhotoVoltaic technologies has faced a lot of structural problems, mostly associated to the increase of geometrical concentration ratio, caused by the reduction of cell area. At the same time the system complexity has grown, therefore it was necessary to enhance reproducibility and scalability of sun tracking systems, thus improving the accuracy of mechanics and controls. Solar troughs are usually employed in thermal applications. The most diffused linear concentrating systems are trough collectors with parabolic profile, which focus the sunlight over a linear absorber placed near their focal position, commonly a metal pipe surrounded by a glass tube. While in the examined case, the main components of the CPV trough are a linear parabolic mirror and an array of PV cells. When the absorber is composed of a PV cells array, this introduces severe requirements on light distribution, which ought to be combined with collection efficiency optimization. Hence the matching between received and collected image becomes a critical element for the performance level and even for the operation of the CPV system. Every PV cell has specific ranges of light levels and light uniformity necessary to reach the high photoelectrical conversion levels foreseen for a good PV system functionality.
The theoretical studies presented in this paper are based on the experimentation performed on a prototype of linear CPV system with parabolic profile. The selected PV cells are characterized by elevated conversion efficiency for illumination in the range of 100-500 Suns. In order to improve the optical performance of a CPV system it is necessary to know how the different optical parameters influence the way the sunlight is concentrated on the receiver [4][5], which in this case consists in a group of high efficiency cells mounted into a linear array.
All analyses of collector optical features are simulated with the optical design software Zemax, considering a source emitting 1 Sun (and a receiver width of 30mm). Within the simulation, it is important to specify the model used for the solar divergence. An improper model for the ray divergence would strongly influence the simulated light distribution over the cells, causing a large error on evaluating the irradiance value. Considering that the sun emits rays in each direction without preferences (it approximates an isotropic source), an elliptical model for the solar divergence was chosen.

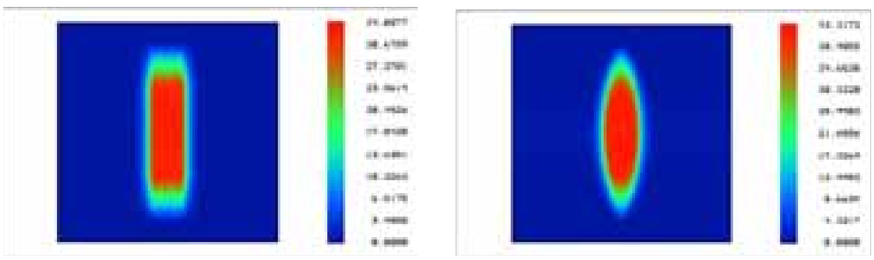

Fig. 1 - Image for rectangular (1a) or elliptical (1b) divergence model.

Just to give an example, Figure 1a-b shows how an inaccurate model in the simulation tools can lead to a big error in the results: two images on the mirror focal plane are reported to compare the effect on image formation for two different divergence models. The shape of the image reflects the angular distribution of source rays: a rectangular divergence model is used in Fig.1a; while an elliptical divergence model is used for Fig.1b.

The first study analyses combinations of collector entrance apertures and focal lengths for a set of parabolic troughs. The collector is modelled starting from a rectangular flat-plate with fixed dimensions 1600mm x 1200mm. The concave mirror can be realised curving the rectangular metal plate, thus giving a series of options for the collector transverse section that correspond to different values of focal length f. The constraint is that the total development of the mirror surface profile remains 1600mm. Among these profiles we have chosen the mirror shape to be realised.

The analysis is based on two foremost requirements: the maximisation of total power on the cell and of irradiance distribution uniformity. The simulation examines the total collected power and its distribution in the focal plane of the collector. All simulations are performed considering a system with a receiver composed of a cooling conductor, with a rectangular transverse section, placed behind the cells. Therefore we take into account the obscuration introduced in the real system by the necessary thermal component.

Some examples of focused image profiles are presented in Fig.2. The figure plots the irradiance distribution over the focal plane; the centre (X=0) is the focal point. The cross section plane (X-axis of Fig.2) is perpendicular to the trough linear axis and corresponds to the plane in which the concentration is performed. A reference size for the rectangular PV cell is indicated on the X-axis: 7mm x 10mm. The focused images are plotted for various focal lengths; then these profiles are integrated on the cross section plane, from the centre towards the borders of the image. The results are shown in Fig.3 as total power versus the lateral dimension of the cell: in the figure two dashed lines indicate two widths corresponding to possible PV cells (7mm x 10mm and 10mm x 10mm). Five focal lengths, are considered and the corresponding collector entrance apertures are: 1507mm, 1528mm, 1543mm, 1562mm, 1573mm, respectively from f=600mm to f=1200mm.

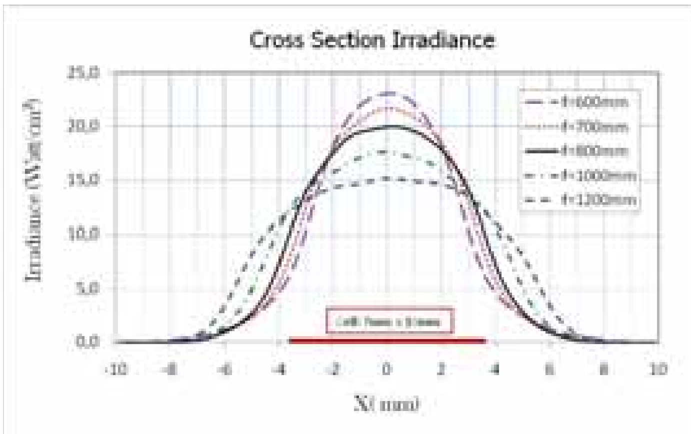

Fig. 2 - Profile of irradiance distribution on the focal plane.

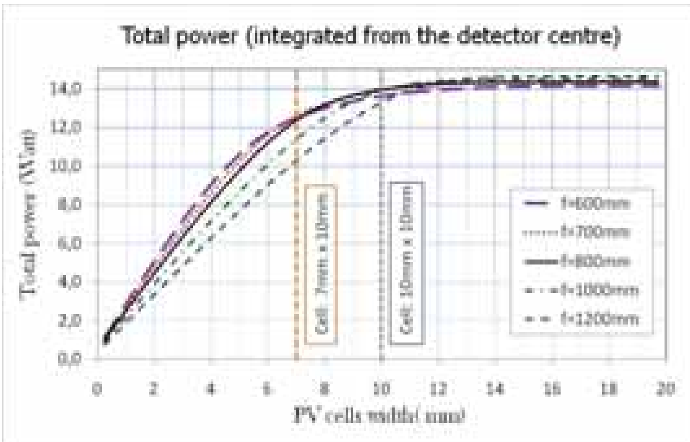

Fig. 3 - Total power concentrated on the receiver.

The best configuration for our aims corresponds to the collector with focal length 800mm and entrance aperture 1543mm x 1200mm (Fig. 4). This choice has been made considering three main reasons. First of all, the difference in irradiance between centre and border points of the cell is minimized (Fig.2): this parameter strongly influences the photovoltaic performance of the cell [1,2]. Since the main purpose is electricity production, the second reason is to have a situation in which the light concentrated on the receiver should maximise the light flux on the cell (Fig.3). At last, in order to limit the action of further mechanical stresses, compact dimensions for the whole structure are preferred (Fig.4).

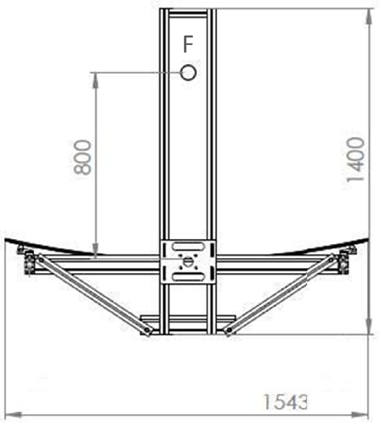

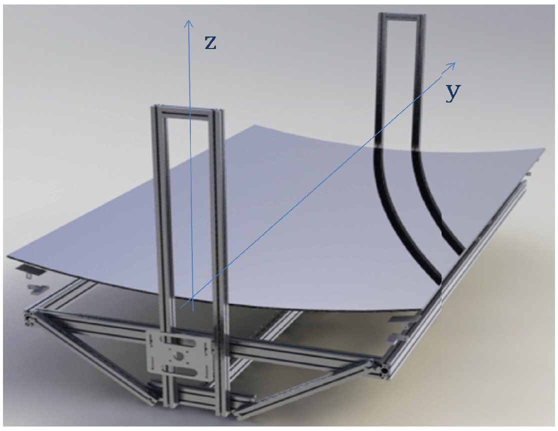

Fig. 4 - Mechanical and geometrical scheme of collector (4a) and shaded model (4b).

3. Effects of receiver defocusing on collected power

The second study investigates the effect of absorber defocusing along the symmetry axis of the parabola. The analysis starts from the practical experimentation, which suggests placing the absorber slightly over the parabola focus. In connection with misalignments and sun tracking precision, it could be useful to know how the shape of irradiance profile varies by shifting the receiver along the parabola axis. The defocusing positions correspond to parallel planes slightly over or under the focal plane. This analysis gives indications about the energy losses in case of errors in the placement of the PV cell. On the other hand, the use of a defocused image can be useful to compensate an imprecise or unstable sun pointing.

Figure 5 shows the results of simulations varying only the position of the test plane for the irradiance profile, neglecting all the other effects such as angular misalignments or mirror deformations. The simulations consider positions parameterised by the displacement from F, at a distance f=800mm: positive Δf for points over F and negative Δf for points under F (the exact focal point F is shown in Fig.4a). The Δf values reported in the label of Fig.5 are in mm.

The simulations evidence symmetry on the displacements: almost the same distribution of light is obtainable for positive or negative shifts of the same length.

The results show that for $|\Delta f| \leq 2$mm the distribution shape is almost identical to the original one, with the receiver in the focal plane. The corresponding decrease in collected power is around 5% (from 92% to 87%). Relevant modifications in the irradiance profile happen starting from $|\Delta f| >$ 4mm (Fig.5).

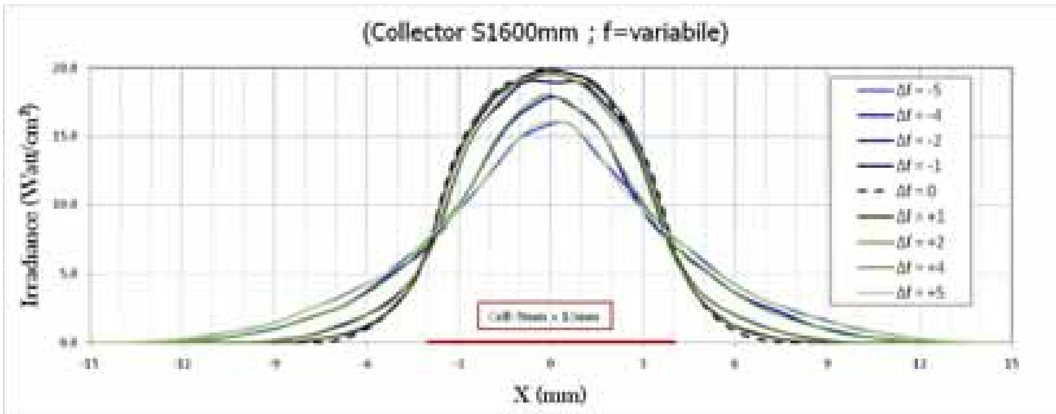

Fig. 5 - Irradiance distribution on the receiver defocused of Δf.

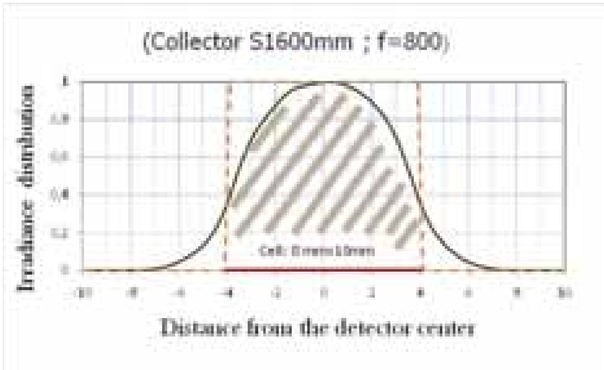

Fig. 6 - Irradiance distribution on the receiver: real (solid line) versus ideal one (dashed line)

The main effect of receiver defocusing is the spreading of the light in the tails of the distribution with a consequently lower curve maximum. Such a situation leads to a reduced amount of light arriving on the cell, which has fixed dimensions (8mm x 10mm). But at the same time the gap in irradiance value, between centre and border of the cell, becomes smaller. In general this gap has to be minimized: because the cells performance increases with the illumination uniformity. The ideal situation would result in concentrating all the light impinging on the primary mirror over the cell, with an irradiance distributed in a square profile, as shown by the red dashed lines in Fig.6.

4. Study of deviations from the parabolic profile

The primary mirror of a parabolic trough can be affected by rigid deformations of the profile. The third study examines profile deformations introducing a mathematical approach to reproduce real mirror profiles. In practice the deformations of a real reflecting surface occur because of mechanical material constraints and structural limitations; moreover in operating conditions some additional deformations can be caused by dynamic stresses such as wind pressure. The technique for rigid deformation reproduction is based on the use of *conic section equation* and *conic constant* *K* to express the collector profile, which is thus described by:

$$z(x) = \frac{\frac{x^2}{R}}{1+\sqrt{1-\frac{(K+1)x^2}{R^2}}} \qquad (1)$$

where *R* is the radius of curvature at x=0, i.e. in the parabola vertex.
The conic constant is related to the *eccentricity e* of the *conic* by the following equation:

$$K = -e^2 \qquad (2)$$

This parameter is an index of the difference between the *conic section* and the circular profile or the parabolic profile.
Another way to individuate the *conic* is by using the curvature *C*:

$$C = \frac{1}{R} \tag{3}$$

The resulting reformulation is:

$$z(x) = \frac{Cx^2}{1+\sqrt{1-(1+K)C^2x^2}} \tag{4}$$

Using one of the mentioned notations, Eq. (1) or Eq. (4), to express a *conic section*, the *K* value completely identifies the curve and it distinguishes among the *conics* as summarised in Table 1.

Table 1 - Summary of the *conics* in dependence of *conic constant K* and *eccentricity e*.

Conic name	Conic constant	Eccentricity
circumference	$K = 0$	$e = 0$
ellipse	$-1 < K < 0$	$0 < e < 1$
parabola	$K = -1$	$e = 1$
hyperbole	$K < -1$	$e > 1$

To reproduce a real case, the simulated collector deviates from the parabolic profile and the deformed mirror profile can be expressed as an *elliptic* or a *hyperbolic* curve. In practice the *K* value of a real mirror can only be approximately assessed. A more realistic parameter is the displacement in the vertical *z* coordinate between the border points of an ideal parabolic section and the real (deformed) profile. This quantity, indicated as Δz, parameterises the rigid deformations of real mirror profiles. Positive Δz correspond to *elliptic* deformations; while negative Δz correspond to *hyperbolic* deformations, as evidenced by Table 2.

A previous analysis, on the mechanical tolerances for our system, individuated as possible range for the fluctuations -3 mm < Δz < 3 mm. However, the relationship between $z(x)$ and K is not linear, so it is not immediate to derive the corresponding constraints for K starting from the limitations for Δz.

To solve this problem, here we provide the details of a numeric procedure, which uses as constraint the development of the *conic* profile and refers to the chosen Δz values.

We define $P_{0,m} = (x_{0,m}, z_{0,m})$ as the border point of the correct parabolic profile, K_0 its *conic constant* (which is -1 for a parabola) and l_0 the length of the semi-parabola arc, which is fixed. Let then $P_{i,m} = (x_{i,m}, z_{i,m})$, K_i and l_i be the same parameters for a generic *conic*, describing the deformed mirror profile.

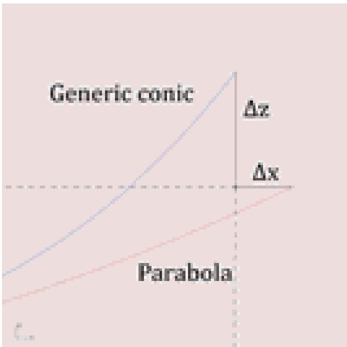

Fig. 7 - Δz definition.

The difference between the two border points, of real mirror profile and ideal parabolic profile will be $\Delta z_{i,m} = |z_{0,m} - z_{i,m}|$.

The following steps describe how the procedure works:

1. first of all, a set of values $\Delta z_i = \Delta z_1, \Delta z_2, \Delta z_3, \ldots$ (in Table 2) are selected, with extremes and step in agreement with system mechanical tolerances and mounting precision;
2. several possible values for K_i are tried forcing the constraint $l_i \cong l_0$, thus imposing that the *conic* profile simulating the deformed mirror has the same length of the parabolic profile;
3. we calculate the border points coordinate $P_{i,m} = (x_{i,m}, z_{i,m})$ and the vertical border distance $\Delta z_{i,m} = |z_{0,m} - z_{i,m}|$. If $\Delta z_{i,m} - \Delta z_i > 0{,}001$, we try again (slightly modifying K_i), returning to the second step in an iterative process.

The accuracy of 0,001mm for *Δz* corresponds to a maximum error for the profile half-length of 0,6mm. By the practical point of view, the level of mechanical precision is not comparable with the mathematical accuracy. By a numerical point of view, the chosen tiny value is necessary to distinguish between the different conics and to attain a more accurate *K* assessment.
The described numerical procedure has been used to reproduce the rigidly deformed profiles. Then the loss in collection efficiency has been simulated for every single profile.
Table 2 shows some significant results for the effects of profile deformations (in column 3) on the collection efficiency (in column 8). Columns 1-7 report the details of the numerical procedure, with the parameters describing the deformed mirror profiles.

Table 2 - Efficiency obtained for different *conics* defined by the *conic constant K*.

Deformation type	Deformation direction	**K**	**Half-Aperture**	**Half-Length**	**Zmax**	**ΔZ**	**Efficiency**
Elliptic	Internal	**-0,6880**	**770,50**	**800,582**	**189,005**	**3,00**	**69%**
	Internal	**-0,7752**	**770,50**	**800,217**	**188,005**	**2,00**	**76%**
	Internal	**-0,8864**	**771,00**	**800,322**	**187,004**	**1,00**	**90%**
	Internal	**-0,9540**	**771,50**	**800,611**	**186,504**	**0,50**	**93%**
	Parabolic profile	**-1**	**771,50**	**800,432**	**186,004**	**0,00**	**93%**
Hyperbolic	External	**-1,0465**	**771,50**	**800,253**	**185,504**	**-0,50**	**92%**
	External	**-1,1161**	**772,00**	**800,545**	**185,003**	**-1,00**	**90%**
	External	**-1,2119**	**772,00**	**800,192**	**184,003**	**-2,00**	**79%**
	External	**-1,3328**	**772,50**	**800,312**	**183,003**	**-3,00**	**69%**

Figure 8 graphically reports the results of collection efficiency versus mirror edge displacement *Δz*, indicating the deformation amount. The rigid deformations of mirror profile cause a reduction in the collection efficiency of the solar trough. The curve in Fig. 8 presents a symmetrical trend for elliptical and hyperbolical deformations, but column 8 of Table 2 evidences that the behaviour is slightly different for the two cases.

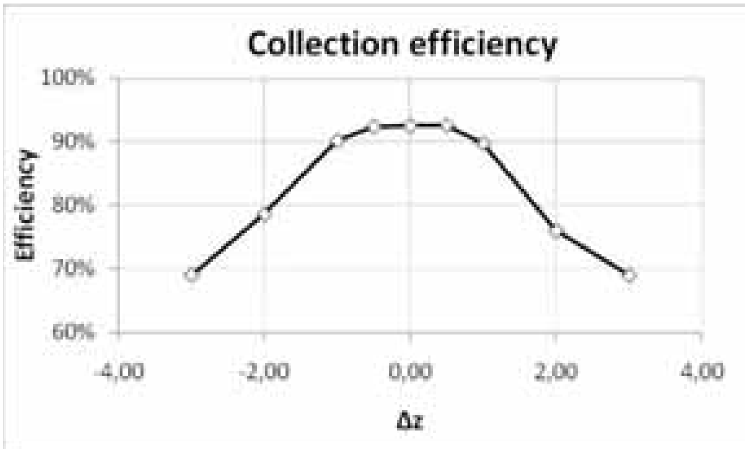

Fig. 8: Collection efficiency for deformed mirrors.

5. Conclusion

Some crucial optical characteristics and performance for parabolic trough photovoltaic/thermal collectors have been discussed. The studies started from a specific configuration corresponding to a trough prototype, which is now under test in operative conditions. The collection efficiency has been evaluated considering an analytical model for the rigid deformation of the primary mirror. The results show that the collection efficiency exceeds 90% for mirror edge displacement Δz around 1mm. In the range of mechanical tolerances admitted for our system (3mm), the efficiency always exceeds 70%.

But the most interesting study concerns the variation in the irradiance profile on the receiving cells. The light distribution over the cell represents a crucial parameter affecting performance level, functionality and consumption of the PV cells. The study examines layouts with different focal lengths (f): the comparison among different configurations allowed us to choose the better solution for our system in terms of irradiance and total power collected on the cells. A dedicated analysis considers the defocusing effects for a specific configuration (f=800 mm). Displacements of the receiver position, with same length but opposite directions (over or under F), have the same effect on the irradiance distribution on the receiver itself. Considerable changes on the irradiance profile occur for displacements of lengths over 4mm.

References

[1] Stuart R. Wenham, Martin A. Green, Muriel E. Watt, Richard Corkish, Applied Photovoltaics, Earthscan Publications Ltd. , 2007

[2] Winston R, Miñano JC, Benítez P, Shatz N, Bortz JC. Nonimaging Optics, Elsevier Academic Press, Amsterdam 2005

[3] Coventry, JS. Performance of a concentrating photovoltaic/thermal solar collector, Solar Energy, Volume 78, Issue 2, February 2005, pp 211-222

[4] Fontani D, Sansoni P, Francini F, Jafrancesco D, Chiani G, De Lucia M. Efficiency of a linear parabolic mirror for geometrical deformations proceedings of EUROSUN 2008 1st International Conference on Solar Heating, Cooling and Buildings, Lisbon - Portugal, 7-10 Oct. 2008

[5] Kandpal TC, Mathur SS, Singhal AK. Optical performance of a composite parabolic trough, Applied Energy, Volume 19, Issue 3, 1985, pp 231-9